

InPK: Infusing Prior Knowledge into Prompt for Vision-Language Models

Shuchang Zhou

University of Electronic Science and Technology of China

sczhou@uestc.edu.cn

Abstract

Prompt tuning has become a popular strategy for adapting Vision-Language Models (VLMs) to zero/few-shot visual recognition tasks. Some prompting techniques introduce prior knowledge due to its richness, but when learnable tokens are randomly initialized and disconnected from prior knowledge, they tend to overfit on seen classes and struggle with domain shifts for unseen ones. To address this issue, we propose the InPK model, which infuses class-specific prior knowledge into the learnable tokens during initialization, thus enabling the model to explicitly focus on class-relevant information. Furthermore, to mitigate the weakening of class information by multi-layer encoders, we continuously reinforce the interaction between learnable tokens and prior knowledge across multiple feature levels. This progressive interaction allows the learnable tokens to better capture the fine-grained differences and universal visual concepts within prior knowledge, enabling the model to extract more discriminative and generalized text features. Even for unseen classes, the learned interaction allows the model to capture their common representations and infer their appropriate positions within the existing semantic structure. Moreover, we introduce a learnable text-to-vision projection layer to accommodate the text adjustments, ensuring better alignment of visual-text semantics. Extensive experiments on 11 recognition datasets show that InPK significantly outperforms state-of-the-art methods in multiple zero/few-shot image classification tasks.

1. Introduction

In recent years, Vision-Language Models (VLMs) pre-trained on large-scale image-text datasets, such as CLIP [25], have shown strong generalization across downstream tasks. To improve model adaptation to specific tasks or datasets, particularly in zero/few-shot settings, the community has proposed many solutions [8, 13, 14, 44, 49, 50]. Among these, prompt tuning [13, 14, 49, 50] has emerged as a popular strategy for adapting VLMs to various visual recognition tasks in zero/few-shot scenarios.

Prompt tuning techniques have gained attention for their ability to improve VLMs' performance on downstream tasks by leveraging textual prompts. For example, CoOp [50] and CoCoOp [49] replace fixed prompts with learnable tokens, achieving substantial improvements through fine-tuning on a limited number of samples. Recent works [11, 13, 14] extend this concept to multimodal prompt tuning, fine-tuning both text and visual branches to improve performance on both base (seen) and novel (unseen) classes. However, since learnable tokens are optimized primarily for the base classes during training, these methods often suffer from overfitting, which leads to domain shifts when encountering novel classes. To address this problem, a line of works [12, 16, 21, 28, 46] introduce prior knowledge to enhance object understanding, helping the model better match visual information with textual descriptions. While these approaches alleviate overfitting to some extent, the random initialization of learnable tokens and their disconnection from prior knowledge (Fig. 1:a (top)) still hinder the model's ability to extract discriminative and generalized features, limiting its performance improvement on both base and novel classes.

To address the aforementioned issue, we strategically infuse the class-specific prior knowledge into learnable tokens at the initialization stage (Fig. 1:a (bottom)) to establish explicit class-relevant preferences and provide higher-quality input to subsequent layers. Furthermore, to prevent the dilution of class information across multi-layer encoders, we continuously reinforce the interaction between learnable tokens and prior knowledge at various feature levels. This progressive design enables the model to more effectively focus on class-relevant details. For base classes, this design reduces overfitting to irrelevant information during training, enhancing the model's ability to perceive fine-grained differences and extract more discriminative text features, thus decreasing the likelihood of misclassification. For novel classes, learnable tokens acquire generalization capabilities through common visual concepts derived from prior knowledge, helping the model infer the appropriate position of novel classes within the existing semantic structure and thereby improving its generalization performance on un-

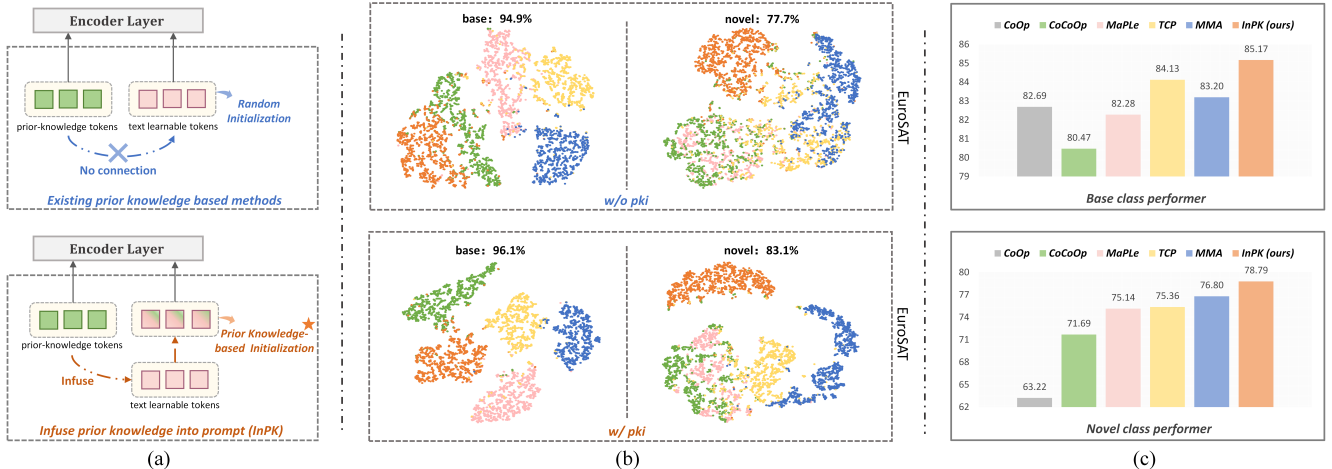


Figure 1. (a) Existing prior knowledge-based prompting techniques initialize learnable tokens randomly, leaving them disconnected from class-specific prior knowledge (illustrated in top). Our approach infuses prior knowledge into learnable tokens before feeding them into the encoder layers each time, providing a prior knowledge-based initialization that explicitly emphasizes class-relevant information (illustrated in bottom). (b) t-SNE visualization of the feature manifolds for our method with and without prior knowledge infusion (pki) on the EuroSAT dataset. Our method with pki shows tighter intra-class distances, indicating enhanced consistency, and larger inter-class distances, reflecting improved class discrimination. (c) In the base-to-base/base-to-novel setting, our method significantly outperforms the state-of-the-art methods regarding average results on 11 recognition datasets.

seen classes. Moreover, while prior knowledge-based methods often prioritize the text branch, they tend to overlook the impact of text adjustments on visual semantic alignment. To address this issue, we introduce a learnable text-to-vision projection layer to enforce stronger alignment between visual and textual semantics.

In this paper, we propose InPK, a novel approach that **infuses prior knowledge into prompt** for vision-language models. The t-SNE visualization results also demonstrate the effectiveness of prior knowledge infusion. (Fig. 1:b). Given the importance of high-quality prior knowledge in enhancing category recognition, and the rich world knowledge inherent in Large Language Models (LLMs), we leverage LLMs to generate comprehensive and discriminative prior knowledge using a predefined instruction template. This knowledge consists of detailed attribute terms that capture subtle class features, refining the model’s understanding of class boundaries. It is then infused into learnable tokens at multiple feature levels, with progressively strengthened interactions, enabling the model to learn more discriminative and generalized features. Moreover, since the text branch incorporates prior knowledge, we introduce a learnable text-to-vision projection layer to adapt to text adjustments, ensuring better alignment between visual and textual semantics. To address potential confusion caused by common attribute words across different categories, we introduce regularization constraints that emphasize the importance of class names, preventing the model from overfitting to shared attributes. Notably, experimental results of average accuracy on 11 popular recognition datasets show that

InPK significantly outperforms state-of-the-art methods on the base and novel classes (Fig. 1:c). The main contributions of this paper include:

- We infuse prior knowledge into learnable tokens across multiple feature levels, guiding the model to extract discriminative and generalized features, therefore improving performance on both base and novel classes.
- We introduce a learnable text-to-vision projection layer to accommodate the text adjustments, enhancing the alignment between visual and textual semantics.
- Our method conducts extensive experiments on 11 popular visual recognition datasets, demonstrating its effectiveness in multiple zero/few-shot image classification tasks.

2. Related Work

2.1. Vision-Language Models

Vision-Language Models (VLMs) represent significant progress in multimodal learning [29–31] in recent years. These models are pre-trained on large-scale datasets to effectively learn joint representations from both images and text. Recent studies [10, 18, 25, 39, 40] have demonstrated VLMs’ superior performance in tasks such as zero/few-shot image recognition. Notably, the pioneering work CLIP [25] is renowned for its simplicity and effectiveness, leveraging large-scale image-text pair training and contrastive learning techniques. Other works like ALIGN [10], FILIP [39], Florence [40], and REACT [18] further highlight VLMs’ strong open vocabulary understanding. To adapt pre-trained

VLMs to specific downstream tasks, numerous task-specific methods have been proposed including segmentation [33, 45, 48], image recognition [1, 32, 36, 37, 43] and object detection [6, 41, 47, 51]. In this work, we propose a novel prompt-tuning technique that enhances VLMs’ generalization performance across various visual recognition tasks.

2.2. Prompt Learning for Vision-Language Models

Fine-tuning Vision-Language Models (VLMs) for downstream tasks or datasets while preserving their original generalization capabilities poses significant challenges. Retraining the entire model is often impractical due to the vast number of parameters, and it risks overfitting, which could diminish the generalization benefits obtained during pre-training. To tackle this, prompt-tuning methods have emerged, with CoOp [50] being a pioneering approach. CoOp adapts VLMs to downstream tasks by introducing learnable vectors in place of hand-crafted prompts. Extensions of this approach [13, 23, 36, 37, 42, 49], multimodal prompt tuning [3, 13, 19] has been applied to fine-tune both text and visual branches simultaneously. To prevent overfitting, a line of works [14, 37, 38, 52] have introduced regularization constraints to reduce the loss of general information. Other approaches, such as UNIGRAM [17] and ProMetaR [23], leverage meta-learning to enhance generalization by initializing prompts or applying regularization in the meta-learning framework. More recently, some methods [12, 16, 21, 28, 46] have introduced external knowledge to enrich textual representations and better capture complex visual semantics. Our approach goes beyond using learnable tokens by infusing them into class-specific prior knowledge to provide class-relevant preferences, resulting in improved generalization performance on downstream tasks.

3. Methodology

In this section, we first provide a brief overview of CLIP [25]. Next, we comprehensively introduce our proposed method InPK.

3.1. Review of CLIP

We build our method on a pre-trained vision-language model CLIP. After feeding the CLIP model an image and its corresponding text description, CLIP employs a contrastive loss to establish global alignment between image and text. CLIP comprises a text encoder θ and an image encoder ϕ , which work together to map the image and text into a shared feature space.

In the visual branch, the input image \mathcal{I} is divided into patches, resulting in $U = \{v_{\text{cls}}, v\}$, where v_{cls} is the class token and v represents the patch embeddings. Subsequently, the sequence U is passed through the image encoder to obtain the visual feature $x = \phi(U)$, where $x \in \mathbb{R}^d$.

In the text branch, the input is defined as $T = \{T_0, c_k\}$, where T_0 represents hand-crafted templates like "a photo of a { }", and c_k denotes the class name for the k -th class. The input T is tokenized into n word embeddings $E = \{e_1, e_2, \dots, e_n\}$, which are then fed sequentially into L transformer layers $\{\theta_i\}_{i=1}^L$:

$$E^i = \theta_i(E^{i-1}) \quad i = 1, 2, \dots, L. \quad (1)$$

Then, the text embedding e_n^L then corresponding to the final token of the last transformer layer is projected into the common vision-language space to obtain the feature $f \in \mathbb{R}^d$:

$$f = Proj(e_n^L). \quad (2)$$

Finally, for zero-shot inference, text prompts are provided with class labels $y \in \{1, 2, \dots, N_c\}$, and the text feature f is matched with the image feature x using the following:

$$p(\hat{y} = i | \mathcal{I}) = \frac{\exp(\text{sim}(x, f_i) / \tau)}{\sum_{k=1}^{N_c} \exp(\text{sim}(x, f_k) / \tau)}, \quad (3)$$

where $\text{sim}(\cdot, \cdot)$ denotes cosine similarity, and τ is the temperature.

3.2. InPK: Infusing Prior Knowledge into Prompt

Based on the CLIP model, to further adapt the VLMs to specific downstream tasks while excelling in both base and novel classes, we propose the InPK model, as depicted in Fig. 2. Different from other methods based on prior knowledge [12, 16, 21, 46], which randomly initialize the learnable tokens, our approach infuses prior knowledge into learnable tokens at the initialization stage and progressively strengthens the connection between prior knowledge and tokens across multiple feature levels. Furthermore, we introduce a learnable text-to-vision projection layer to accommodate text adjustments and enforce alignment between visual and textual semantics. Finally, regularization constraint is employed with the objective of retaining general knowledge and emphasizing the role of class names.

3.2.1. Generation of Prior Knowledge

Regarding prior knowledge, relying solely on class names, especially for rare or ambiguous scientific terms, limits the model’s ability to effectively associate these terms with visual information. Therefore, it is essential to incorporate attribute words related to each category alongside the class names. In our method, prior knowledge includes both class names and class-specific attributes, enriching the model’s semantic understanding and universal visual concepts brought by attributes that provide cross-class knowledge. We generate attribute words using GPT-4, leveraging its rich world knowledge and guide the process with a predefined instruction template that incorporates both

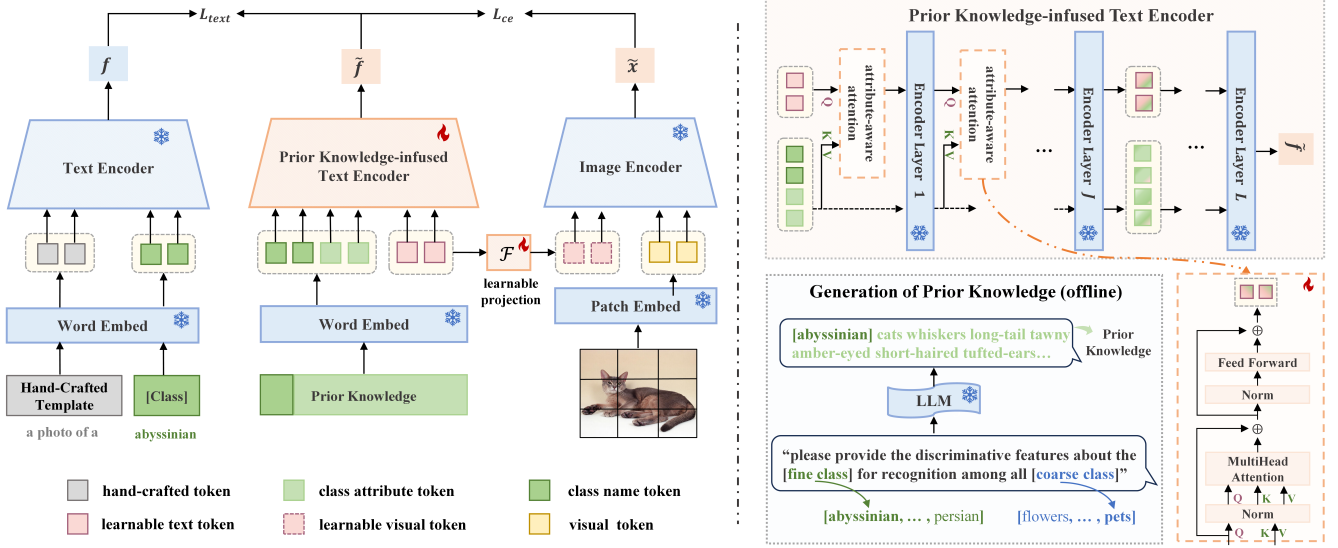


Figure 2. Overview of InPK method. Prior knowledge is generated offline using a predefined instruction template and subsequently fed into the **P**rior **K**nowledge-**i**nfused text encoder (PKi). Within PKi, class-specific prior knowledge is infused into learnable tokens through attribute-aware attention at the initialization stage, and the interaction between tokens and prior knowledge is progressively reinforced across multiple feature levels. Meanwhile, we introduce a learnable text-to-vision projection layer to better align visual-text semantics. Furthermore, loss L_{text} is applied to mitigate the model’s forgetting of general information and to emphasize the role of class names.

the class name (fine-grained) and dataset name (coarse-grained). The template is as follows: “Please provide the discriminative features about the [fine class] for recognition among all [coarse class]”. This process yields the input $G = \{c_k, g_1, \dots, g_N\}$, where c_k denotes the class name for the k -th class, and $\{g_1, \dots, g_N\}$ represent N attribute words. Prior knowledge is generated offline, eliminating the need for training or inference time. Samples of these attribute words are provided in the supplementary material.

3.2.2. Prior Knowledge-infused Text Encoder

With the acquired class-specific prior knowledge, we avoid merely concatenating the learnable tokens with prior knowledge before feeding them into the text encoder. Instead, our approach infuses the prior knowledge into the learnable tokens, introducing explicit category preference and delivering higher-quality input to subsequent layers. Therefore, beyond the original feature f derived from hand-crafted prompts in the text branch, we introduce an additional pathway within the PKi module that incrementally models features, ultimately producing the new textual feature \tilde{f} . Specifically, the input tokens for the PKi module are structured as $\{P_t, \tilde{E}\}$, where $P_t = \{p_t^1, p_t^2, \dots, p_t^M\}$ consists of M learnable tokens, and $\tilde{E} = \{\tilde{e}_1, \tilde{e}_2, \dots, \tilde{e}_n\}$ represents the word embeddings of G . We then introduce an attribute-aware attention mechanism that fuses class-specific knowledge with the learnable tokens. In this mechanism, the learnable tokens P_t serve as the query Q , while the class-specific prior knowledge embeddings \tilde{E} as both the key K and the value V , resulting in a robust token em-

bedding \widehat{P}_t that incorporates prior knowledge:

$$A = MultiHead(LN(P_t), LN(\tilde{E}), LN(\tilde{E})) + P_t, \quad (4)$$

$$\widehat{P}_t = FFN(LN(A)) + A, \quad (5)$$

where $MultiHead()$ and $FFN()$ follow the standard Transformer configurations [27], representing multi-head attention and feed-forward neural network, respectively. Layer normalization (LN) is applied before each block. Furthermore, to counteract the potential dilution of category information caused by multi-layer encoders, we incorporate attribute-aware attention into each transformer layer of the PKi up to a specific depth J , allowing for step-by-step feature modeling. Specifically, the PKi itself comprises L layers of frozen transformers, with all parameters pre-trained. The fused learnable token \widehat{P}_t^i is concatenated with the E^i , and the resulting tokens are then passed to the $(i + 1)^{th}$ transformer layer:

$$[P_t^i, \tilde{E}^i] = \theta_i([\widehat{P}_t^{i-1}, \tilde{E}^{i-1}]) \quad i = 1, 2, \dots, J, \quad (6)$$

where $[\cdot, \cdot]$ refers to concatenation operation and the θ_i is the i^{th} transformer layer in text Encoder. After J^{th} transformer layer, the tokens are fed into the remaining layers and obtain the final text feature $\tilde{f} \in \mathbb{R}^d$:

$$[P_t^j, \tilde{E}^j] = \theta_j([P_t^{j-1}, \tilde{E}^{j-1}]) \quad j = J + 1, \dots, L, \quad (7)$$

$$\tilde{f} = Proj(\tilde{e}_n^L). \quad (8)$$

3.2.3. Alignment of Text and Visual Branches

Due to the adjustment of the text branch, where additional prior knowledge is introduced, we propose a trainable text-to-vision projection layer \mathcal{F} to better align visual and textual semantics. The textual learnable tokens \mathbf{P}_t are passed through this projection layer to generate the corresponding visual learnable tokens \mathbf{P}_v . The text and visual branches are dynamically adjusted using cross-modal shared parameters, ensuring consistent alignment between the two modalities. The specific formula is as follows:

$$\mathbf{P}_v = \mathcal{F}(\mathbf{P}_t), \quad (9)$$

where $\mathbf{P}_v = \{\mathbf{p}_v^1, \mathbf{p}_v^2, \dots, \mathbf{p}_v^M\}$ consists of M learnable visual tokens. By combining the fixed token \mathbf{U} obtained from CLIP, we define the token of the new visual branch as $\mathbf{V} = \{\mathbf{U}, \mathbf{P}_v\}$. Then, the visual token \mathbf{V} is passed through the image encoder to obtain new visual features $\tilde{\mathbf{x}} = \phi(\mathbf{V})$, where $\tilde{\mathbf{x}} \in \mathbb{R}^d$.

3.2.4. Training Objective

In the new text and visual branches, text features $\tilde{\mathbf{f}}$ and visual features $\tilde{\mathbf{x}}$ are obtained. Thus, the prediction probability for \mathcal{I} pertaining to label i is represented as:

$$p(\hat{y} = i | \mathcal{I}) = \frac{\exp\left(\text{sim}\left(\tilde{\mathbf{x}}, \tilde{\mathbf{f}}_i\right) / \tau\right)}{\sum_{k=1}^{N_c} \exp\left(\text{sim}\left(\tilde{\mathbf{x}}, \tilde{\mathbf{f}}_k\right) / \tau\right)}, \quad (10)$$

where $\text{sim}(\cdot, \cdot)$ denotes the cosine similarity, τ is a temperature parameter that controls the sharpness of the softmax distribution, and N_c the number of seen classes. Thus, the cross-entropy loss between the true label and the predicted label is minimized as follows:

$$\mathcal{L}_{ce} = -\frac{1}{N} \sum_{i=1}^N \log(P(\hat{y} = y_i | \mathcal{I}_i)), \quad (11)$$

where N represents the number of samples in the training dataset, y_i denotes the ground-truth label of image \mathcal{I}_i .

Furthermore, the attribute words of different categories are often generic. For example, Felidae species such as the cat and tiger share common fine-grained attributes, including the presence of whiskers, a long tail, and so on. The constraints of \mathcal{L}_{ce} alone would cause the prompt to become largely dependent on the attribute words, potentially confusing the categories. It is therefore necessary to enhance the role of class names by leveraging the differences of class names within the general text features \mathbf{f} . Following the PromptSRC [14] approach, we introduce a regularization constraint using the $L1$ Loss on the prompted textual features $\tilde{\mathbf{f}}$ to ensure their consistency with the CLIP pre-trained features \mathbf{f} . This regularization prevents the model from overfitting to overly generic or misleading attributes, ensuring that the generated features align with the

pre-trained model’s feature space, without consuming additional inference time. The loss is minimized as follows:

$$\mathcal{L}_{text} = \sum_{i=1}^d \left| \tilde{\mathbf{f}} - \mathbf{f} \right|. \quad (12)$$

The overall training objective becomes:

$$\mathcal{L} = \mathcal{L}_{ce} + \lambda \mathcal{L}_{text}, \quad (13)$$

where λ is a hyperparameter set to 25.0.

4. Experiments

4.1. Experimental Setup

We follow the experimental setting [50] of previous methods to conduct experiments through three evaluation protocols: base-to-novel generalization, few-shot learning, and cross-dataset evaluation.

Base-to-novel generalization. Following the settings of previous methods, we divide the dataset into base and novel classes. The model is trained on a small number of samples from the base classes, and its performance is evaluated on both the base and novel classes. To assess the trade-off between base and novel class performance and verify the generalization capability of the method, we introduce the harmonic mean (HM) [34], which balances accuracy across the two class sets.

Few-shot classification. To evaluate the model’s ability to learn with extremely limited supervision, we assess its performance across few-shot scenarios. Specifically, the model is trained on a small number of labeled images (4-shot) and evaluated on a dataset containing the same classes as those in the training samples.

Cross-dataset evaluation. This setting aims to verify the model’s zero-shot capability in a cross-dataset context. Specifically, the model undergoes few-shot training on the ImageNet-1K dataset and is then directly evaluated on other datasets without further fine-tuning.

Dataset. To comprehensively evaluate our model in various settings, we test our method on 11 image classification datasets, covering a range of tasks. These include general object recognition datasets: ImageNet [5] and Caltech101 [7]; fine-grained classification datasets: OxfordPets [24], StanfordCars [15], Flowers102 [22], Food101 [2], and FGVC Aircraft [20]; scene recognition dataset: SUN397 [35]; action recognition dataset: UCF101 [26]; texture classification dataset: DTD [4]; and satellite imagery dataset: EuroSAT [9].

Experiment detail. Our implementation is based on the code of CoOp [50]. All experiments are fine-tuned using the CLIP model with a ViT-B/16 backbone where $d = 512$, and the results are averaged over three runs with different random seeds (1/2/3). For more experimental details, please refer to the supplementary material.

Method	Base	Novel	HM
CoOp	82.69	63.22	71.66
CoCoOp	80.47	71.69	75.83
TCP	84.13	75.36	79.51
Ours	85.17	78.79	81.85
Δ	+1.04	+3.43	+2.34

(a) Average over 11 datasets.

Method	Base	Novel	HM
CoOp	93.67	95.29	94.47
CoCoOp	95.20	97.69	96.43
TCP	94.67	97.20	95.92
Ours	94.67	97.63	96.13
Δ	+0.00	+0.43	+0.21

(d) OxfordPets

Method	Base	Novel	HM
CoOp	88.33	82.26	85.19
CoCoOp	90.70	91.29	90.99
TCP	90.57	91.37	90.97
Ours	90.10	91.57	90.83
Δ	-0.47	+0.20	-0.14

(g) Food101

Method	Base	Novel	HM
CoOp	79.44	41.18	54.24
CoCoOp	77.01	56.00	64.85
TCP	82.77	58.07	68.25
Ours	84.43	71.30	77.31
Δ	+1.66	+13.23	+9.06

(j) DTD

Method	Base	Novel	HM
CoOp	76.47	67.88	71.92
CoCoOp	75.98	70.43	73.10
TCP	77.27	69.87	73.38
Ours	77.60	71.37	74.35
Δ	+0.33	+1.50	+0.97

(b) ImageNet

Method	Base	Novel	HM
CoOp	78.12	60.40	68.13
CoCoOp	70.49	73.59	72.01
TCP	80.80	74.13	77.32
Ours	81.97	76.10	78.93
Δ	+1.17	+1.97	+1.60

(e) StanfordCars

Method	Base	Novel	HM
CoOp	98.00	89.81	93.73
CoCoOp	97.96	93.81	95.84
TCP	98.23	94.67	96.42
Ours	98.67	94.30	96.44
Δ	+0.44	-0.37	+0.02

(c) Caltech101

Method	Base	Novel	HM
CoOp	80.60	65.89	72.51
CoCoOp	79.74	76.86	78.27
TCP	82.63	78.20	80.35
Ours	82.77	81.13	81.94
Δ	+0.14	+2.93	+1.59

(i) SUN397

Method	Base	Novel	HM
CoOp	97.60	59.67	74.06
CoCoOp	94.87	71.75	81.71
TCP	97.73	75.57	85.23
Ours	98.17	81.27	88.92
Δ	+0.44	+5.70	+3.69

(f) Flowers102

Method	Base	Novel	HM
CoOp	40.44	22.30	28.75
CoCoOp	33.41	23.71	27.74
TCP	41.97	34.43	37.83
Ours	45.67	36.50	40.57
Δ	+3.70	+2.07	+2.75

(h) FGVCaircraft

Method	Base	Novel	HM
CoOp	92.19	54.74	68.69
CoCoOp	87.49	60.04	71.21
TCP	91.63	74.73	82.32
Ours	95.70	82.37	88.54
Δ	+4.07	+7.64	+6.21

(k) EuroSAT

Method	Base	Novel	HM
CoOp	84.69	56.05	67.46
CoCoOp	82.33	73.45	77.67
TCP	87.13	80.77	83.83
Ours	87.13	83.10	85.07
Δ	+0.00	+2.33	+1.24

(l) UCF101

Table 1. Comparison with CoOp, CoCoOp and TCP in the base-to-novel generalization setting. HM: harmonic mean. The best results for each column are highlighted in **bold** font, and the improvement of our method over the SOTA method TCP is indicated as Δ . Our method exhibits outstanding performance in both base and novel classes.

	CoOp [50] (IJCV22)	CoCoOp [49] (CVPR22)	PromptSRC [14] (ICCV23)	MaPLe [13] (CVPR23)	MMA [36] (CVPR24)	TCP [38] (CVPR24)	HPT [28] (AAAI24)	ProMetaR [23] (CVPR24)	Ours
Base	82.69	80.47	84.26	82.28	83.20	84.13	84.32	84.39	85.17
Novel	63.22	71.69	76.10	75.14	76.80	75.36	76.86	76.93	78.79
HM	71.66	75.83	79.97	78.55	79.87	79.51	80.23	80.49	81.85

Table 2. Comparison between our method and the existing state-of-the-art methods in the base-to-novel generalization setting. Our method achieves the best accuracy in both base and novel classes, demonstrating the strong generalization ability of our method.

4.2. Base-to-Novel Generalization

Tab. 1 presents the performance of InPK across 11 recognition datasets in the base-to-novel generalization setting. We implement all methods using a few-shot training approach, with 16 randomly sampled shots per base class. Compared to the recently proposed method TCP [38], our approach shows enhanced performance on 10 out of 11 datasets in terms of harmonic mean (HM), with only a slight drop in performance on the Food101 dataset relative to method TCP. For the average result, since we infuse class-specific

prior knowledge into learnable tokens in Pki, these tokens are expected to learn the common features shared across modalities. This allows our method to perform better on novel class, improving the average accuracy of novel class by 3.43%. Additionally, InPK maintains strong performance on the base class as it can infer more discriminative text features, with an increase of 1.04% in accuracy. When considering both base and novel classes, InPK achieves an absolute average gain of 2.34% over TCP in terms of HM, demonstrating an effective balance between in-domain and out-of-domain data performance.

Method	ImNet	Caltech	Pets	Cars	Flowers	Food	Aircraft	SUN397	DTD	EuroSAT	UCF	Average
CoOp	66.70	93.30	89.40	65.70	70.70	85.90	24.90	62.60	44.30	48.30	67.60	65.37
CoCoOp	70.55	94.98	93.01	69.10	82.56	86.64	30.87	70.50	54.79	63.83	74.99	71.98
PromptSRC	70.80	94.77	93.23	71.83	91.31	86.06	32.80	72.80	60.64	75.02	79.35	75.33
MaPLe	70.67	94.30	92.05	68.70	80.80	86.90	29.03	71.47	54.73	54.87	73.70	70.66
TCP	70.48	95.00	91.90	76.30	94.40	85.30	36.20	72.11	63.97	77.43	80.83	76.72
Ours	71.00	95.00	92.90	77.57	93.27	86.10	36.23	73.73	64.77	83.20	80.30	77.64

Table 3. Comparison of our method with existing methods in the few-shot learning setting. All models are trained with 4-shot samples. Our method shows competitive performance in few-shot learning, achieving the highest average results.

Method	Source	Target										
	ImNet	Caltech	Pets	Cars	Flowers	Food	Aircraft	SUN397	DTD	EuroSAT	UCF	Average
CoOp	71.51	93.70	89.14	64.51	68.71	85.30	18.47	64.15	41.92	46.39	66.55	63.88
CoCoOp	71.02	94.43	90.14	65.32	71.88	86.06	22.94	67.36	45.73	45.37	68.21	65.74
PromptSRC	71.27	93.60	90.25	65.70	70.25	86.15	23.90	67.10	46.87	45.50	68.75	65.81
MaPLe	70.72	93.53	90.49	65.57	72.23	86.20	24.74	67.01	46.49	48.06	68.69	66.30
MMA	71.00	93.80	90.30	66.13	72.07	86.12	25.33	68.17	46.57	49.24	68.32	66.61
TCP	71.40	93.97	91.25	64.69	71.21	86.69	23.45	67.15	44.35	51.45	68.73	66.29
ProMetaR	71.29	93.74	90.59	65.83	71.13	86.39	24.78	67.41	47.08	45.02	69.50	66.61
Ours	71.77	94.47	91.83	65.20	77.17	86.17	27.07	70.60	59.40	52.80	74.27	69.90

Table 4. Comparison of InPK and existing methods in cross-data evaluation settings. All models are trained with 16-shot samples on the source dataset ImageNet and evaluated on 10 other datasets. Our method achieves the highest average accuracy, indicating that InPK has excellent robustness to different data distributions.

Tab. 2 presents a comparison of the average performance of our method against more recent prompt-tuning methods across 11 datasets. The results evident that our method outperforms other methods on both base and novel classes, which demonstrates that the InPK not only maintains excellent recognition accuracy on base class but also exhibits strong generalization capabilities for novel class.

4.3. Few-Shot Learning

Tab. 3 shows the performance of InPK in few-shot learning across 11 datasets. Our method achieves the highest gains on most datasets (7 out of 11). Compared to the best existing method TCP, our model achieves an average improvement of 0.92%. Since InPK introduces class prior knowledge, it compensates for the small number of samples by utilizing this prior knowledge as additional useful information, enhancing the model’s perception of fine-grained differences. This demonstrates that InPK maintains high performance even in limited data scenarios.

4.4. Cross-Dataset Evaluation

To further verify the generalization ability of the model, we evaluate the model and state-of-the-art methods in a cross-data setting. As shown in Tab. 4, our model exhibits outstanding generalization on 8 out of the 10 datasets, with a significant improvement over other methods. The average accuracy reaches 69.90%, demonstrating strong robustness across varying data distributions. This is because the model

infuses the prior knowledge into learnable tokens at various feature levels, which guides the model to focus on category information and better discover latent representations of novel class attributes, thereby improving the model’s performance on unseen classes.

4.5. Ablation Study

Impact of prompt length. We study the effect of prompt length M on model performance in a base-to-novel generalization setting. As shown in Fig. 3 (left), changing M has minimal impact on base class performance. However, for the novel class, performance improves as the prompt length increases. Ultimately, we select $M = 6$, which yields the highest harmonic mean (HM) accuracy, as the optimal prompt length for the model.

Impact of the number of attribute words. We analyze the impact of the number of attribute words N on model performance in the base-to-novel generalization setting as shown in Fig. 3 (right). By varying the number of attribute words, we observe the accuracy of the base class, new class, and harmonic mean (HM). Overall, as the number of attribute words increases, the HM index gradually improves. This is because richer class-specific textual knowledge provides more comprehensive supervision for the model. Notably, when the number of attribute words $N = 25$, the HM value is the highest, indicating that this amount of detailed prior knowledge optimizes the balance between base and novel class performance.

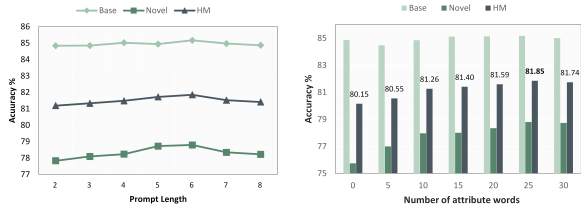


Figure 3. Ablation on prompt depth (left) and the number of attribute words (right).

Impact of inserting attribute-aware attention into different Transformer layers. Tab. 5 presents the analysis of inserting attribute-aware attention into different Transformer layers within PKi in the base-to-new generalization setting. The results indicate that even with $J = 1$, where attribute-aware attention is only applied in the initialization stage, the model’s performance shows a significant improvement. This highlights the importance of providing a prior knowledge-based initialization for the learnable tokens. The model performance is observed to improve with the increase of the prompt depth of module insertion, which can be attributed to the fact that class-specific prior knowledge is able to reduce the loss of category information. Additionally, inserting attribute-aware attention beyond the ninth layer decreases performance, likely because earlier layers have already captured high-level features. Further insertions may interfere with these representations, making the model overly sensitive and reducing its generalization ability. The optimal result is obtained by incorporating attribute-aware attention into the transformer layers up to a depth $J = 9$.

Layer	{1}	{1-3}	{1-6}	{1-9}	{1-12}
Base	84.91	85.10	85.06	85.17	85.02
Novel	78.21	78.39	78.53	78.79	78.82
HM	81.42	81.61	81.66	81.85	81.80

Table 5. Impact of insert layers.

Analysis of model components. We conduct a comprehensive analysis of the key components of InPK, as illustrated in Tab. 6. In this analysis, *Know.* represents the input attribute words, *Attn.* refers to the attribute-aware attention, and *Proj.* represents the learnable projection layer from text prompt to visual prompt. In the text branch, when only class-specific prior knowledge is applied, the model exhibits improvement with an average gain from 79.03% to 80.69% due to the additional supervision provided by the rich attribute information. On the other hand, when only attribute-aware attention is used, the model strikes a better balance between base and novel classes with an average improvement of 0.92%. When both components (*Know.* and *Attn.*) are incorporated together, the model achieves substantial gains across both base and new classes (83.70% vs 85.17%, 74.86% vs 78.79%). In the visual branch, incor-

porating the projection layer improves the HM accuracy by 1.05% compared to the setup without the projection layer. This gain is primarily due to the projection layer’s ability to enhance consistency between the image and text semantics, further optimizing cross-modal alignment.

Text encoder		Image encoder		Base	Novel	HM
<i>Know.</i>	<i>Attn.</i>	<i>Proj.</i>				
✗	✗	✓		83.70	74.86	79.03
✓	✗	✓		83.63	77.95	80.69
✗	✓	✓		84.86	75.94	80.15
✓	✓	✗		84.17	77.70	80.80
✓	✓	✓		85.17	78.79	81.85

Table 6. Ablation on attribute words, attribute-aware attention and learnable text-to-vision projection layer in InPK.

Effectiveness of prior knowledge infusion. To further assess the impact of prior knowledge infusion (pki) into learnable tokens, we apply pki only before the first encoder layer in method CoOp [50], KgCoOp [37], and PromptSRC [14]. As shown in Tab. 7, all three methods exhibit significant improvement, confirming the effectiveness of pki.

Method	Base	Novel	HM
CoOp	82.69	63.22	71.66
+ pki	82.71^{+0.02}	71.42^{+8.20}	76.65^{+4.99}
KgCoOp	80.73	73.60	77.00
+ pki	84.16^{+3.43}	77.93^{+4.33}	80.93^{+3.93}
PromptSRC	84.26	76.10	79.97
+ pki	85.15^{+0.89}	78.60^{+2.50}	81.74^{+1.77}

Table 7. Comparison of baseline methods with and without pki in the base-to-novel generalization setting. ‘pki’ denotes prior knowledge infusion into learnable tokens before feeding them into the encoder layer.

5. Conclusion

In this paper, we have proposed InPK to tackle the issue of prompt-tuning methods overfitting to seen classes and experiencing domain shifts on unseen ones. We infuse class-specific prior knowledge into the learnable tokens at the initialization stage and progressively reinforce their interaction with prior knowledge across multiple feature levels. InPK guides the model to focus on class-relevant information, allowing learnable tokens to capture the fine-grained differences and universal visual concepts within prior knowledge more effectively, thereby enabling the model to extract more discriminative and generalized text features. Furthermore, we introduce a learnable text-to-vision projection layer to accommodate text adjustments, enhancing visual-text alignment. Our method has demonstrated strong performance across 11 recognition datasets, outperforming state-of-the-art approaches in base-to-novel generalization, few-shot learning, and cross-dataset evaluation tasks.

References

- [1] Jean-Baptiste Alayrac, Jeff Donahue, Pauline Luc, Antoine Miech, Iain Barr, Yana Hasson, Karel Lenc, Arthur Mensch, Katherine Millican, Malcolm Reynolds, et al. Flamingo: a visual language model for few-shot learning. *NeurIPS*, 35: 23716–23736, 2022. [3](#)
- [2] Lukas Bossard, Matthieu Guillaumin, and Luc Van Gool. Food-101—mining discriminative components with random forests. In *ECCV*, pages 446–461. Springer, 2014. [5](#)
- [3] Eulrang Cho, Jooyeon Kim, and Hyunwoo J Kim. Distribution-aware prompt tuning for vision-language models. In *ICCV*, pages 22004–22013, 2023. [3](#)
- [4] Mircea Cimpoi, Subhansu Maji, Iasonas Kokkinos, Sammy Mohamed, and Andrea Vedaldi. Describing textures in the wild. In *CVPR*, pages 3606–3613, 2014. [5](#)
- [5] Jia Deng, Wei Dong, Richard Socher, Li-Jia Li, Kai Li, and Li Fei-Fei. Imagenet: A large-scale hierarchical image database. In *CVPR*, pages 248–255. Ieee, 2009. [5](#)
- [6] Ruohuan Fang, Guansong Pang, and Xiao Bai. Simple image-level classification improves open-vocabulary object detection. In *Proceedings of the AAAI Conference on Artificial Intelligence*, pages 1716–1725, 2024. [3](#)
- [7] Li Fei-Fei, Rob Fergus, and Pietro Perona. Learning generative visual models from few training examples: An incremental bayesian approach tested on 101 object categories. In *CVPRW*, pages 178–178. IEEE, 2004. [5](#)
- [8] Peng Gao, Shijie Geng, Renrui Zhang, Teli Ma, Rongyao Fang, Yongfeng Zhang, Hongsheng Li, and Yu Qiao. Clip-adapter: Better vision-language models with feature adapters. *IJCV*, 132(2):581–595, 2024. [1](#)
- [9] Patrick Helber, Benjamin Bischke, Andreas Dengel, and Damian Borth. Eurosat: A novel dataset and deep learning benchmark for land use and land cover classification. *JSTARS*, 12(7):2217–2226, 2019. [5](#)
- [10] Chao Jia, Yinfei Yang, Ye Xia, Yi-Ting Chen, Zarana Parekh, Hieu Pham, Quoc Le, Yun-Hsuan Sung, Zhen Li, and Tom Duerig. Scaling up visual and vision-language representation learning with noisy text supervision. In *ICML*, pages 4904–4916. PMLR, 2021. [2](#)
- [11] Menglin Jia, Luming Tang, Bor-Chun Chen, Claire Cardie, Serge Belongie, Bharath Hariharan, and Ser-Nam Lim. Visual prompt tuning. In *ECCV*, pages 709–727. Springer, 2022. [1](#)
- [12] Baoshuo Kan, Teng Wang, Wenpeng Lu, Xiantong Zhen, Weili Guan, and Feng Zheng. Knowledge-aware prompt tuning for generalizable vision-language models. In *CVPR*, pages 15670–15680, 2023. [1](#), [3](#)
- [13] Muhammad Uzair Khattak, Hanoona Rasheed, Muhammad Maaz, Salman Khan, and Fahad Shahbaz Khan. Maple: Multi-modal prompt learning. In *CVPR*, pages 19113–19122, 2023. [1](#), [3](#), [6](#)
- [14] Muhammad Uzair Khattak, Syed Talal Wasim, Muzammal Naseer, Salman Khan, Ming-Hsuan Yang, and Fahad Shahbaz Khan. Self-regulating prompts: Foundational model adaptation without forgetting. In *ICCV*, pages 15190–15200, 2023. [1](#), [3](#), [5](#), [6](#), [8](#)
- [15] Jonathan Krause, Michael Stark, Jia Deng, and Li Fei-Fei. 3d object representations for fine-grained categorization. In *ICCVW*, pages 554–561, 2013. [5](#)
- [16] Gun Lee, Subin An, Sungyong Baik, and Soochahn Lee. Coapt: Context attribute words for prompt tuning. *arXiv preprint arXiv:2407.13808*, 2024. [1](#), [3](#)
- [17] Juncheng Li, Minghe Gao, Longhui Wei, Siliang Tang, Wenqiao Zhang, Mengze Li, Wei Ji, Qi Tian, Tat-Seng Chua, and Yueting Zhuang. Gradient-regulated meta-prompt learning for generalizable vision-language models. In *ICCV*, pages 2551–2562, 2023. [3](#)
- [18] Haotian Liu, Kilho Son, Jianwei Yang, Ce Liu, Jianfeng Gao, Yong Jae Lee, and Chunyuan Li. Learning customized visual models with retrieval-augmented knowledge. In *CVPR*, pages 15148–15158, 2023. [2](#)
- [19] Xin Liu, Jiamin Wu, Wenfei Yang, Xu Zhou, and Tianzhu Zhang. Multi-modal attribute prompting for vision-language models. *IEEE TCSVT*, 2024. [3](#)
- [20] Subhansu Maji, Esa Rahtu, Juho Kannala, Matthew Blaschko, and Andrea Vedaldi. Fine-grained visual classification of aircraft. *arXiv preprint arXiv:1306.5151*, 2013. [5](#)
- [21] Sachit Menon and Carl Vondrick. Visual classification via description from large language models. *arXiv preprint arXiv:2210.07183*, 2022. [1](#), [3](#)
- [22] Maria-Elena Nilsback and Andrew Zisserman. Automated flower classification over a large number of classes. In *ICVGIP*, pages 722–729. IEEE, 2008. [5](#)
- [23] Jinyoung Park, Juyeon Ko, and Hyunwoo J Kim. Prompt learning via meta-regularization. In *CVPR*, pages 26940–26950, 2024. [3](#), [6](#)
- [24] Omkar M Parkhi, Andrea Vedaldi, Andrew Zisserman, and CV Jawahar. Cats and dogs. In *CVPR*, pages 3498–3505. IEEE, 2012. [5](#)
- [25] Alec Radford, Jong Wook Kim, Chris Hallacy, Aditya Ramesh, Gabriel Goh, Sandhini Agarwal, Girish Sastry, Amanda Askell, Pamela Mishkin, Jack Clark, et al. Learning transferable visual models from natural language supervision. In *ICML*, pages 8748–8763. PMLR, 2021. [1](#), [2](#), [3](#)
- [26] Khurram Soomro, Amir Roshan Zamir, and Mubarak Shah. A dataset of 101 human action classes from videos in the wild. *Center for Research in Computer Vision*, 2(11):1–7, 2012. [5](#)
- [27] A Vaswani. Attention is all you need. *NeurIPS*, 2017. [4](#)
- [28] Yubin Wang, Xinyang Jiang, De Cheng, Dongsheng Li, and Cairong Zhao. Learning hierarchical prompt with structured linguistic knowledge for vision-language models. In *AAAI*, pages 5749–5757, 2024. [1](#), [3](#), [6](#)
- [29] Jiwei Wei, Xing Xu, Yang Yang, Yanli Ji, Zheng Wang, and Heng Tao Shen. Universal weighting metric learning for cross-modal matching. In *CVPR*, pages 13005–13014, 2020. [2](#)
- [30] Jiwei Wei, Xing Xu, Zheng Wang, and Guoqing Wang. Meta self-paced learning for cross-modal matching. In *ACM MM*, pages 3835–3843, 2021.
- [31] Jiwei Wei, Yang Yang, Xing Xu, Xiaofeng Zhu, and Heng Tao Shen. Universal weighting metric learning for

- cross-modal retrieval. *IEEE TPAMI*, 44(10):6534–6545, 2022. 2
- [32] Jiwei Wei, Yang Yang, Xiang Guan, Xing Xu, Guoqing Wang, and Heng Tao Shen. Runge-kutta guided feature augmentation for few-sample learning. *IEEE TMM*, 2024. 3
- [33] Monika Wysoczańska, Michaël Ramamonjisoa, Tomasz Trzciniński, and Oriane Siméoni. Clip-diy: Clip dense inference yields open-vocabulary semantic segmentation for-free. In *CVPR*, pages 1403–1413, 2024. 3
- [34] Yongqin Xian, Bernt Schiele, and Zeynep Akata. Zero-shot learning—the good, the bad and the ugly. In *CVPR*, pages 4582–4591, 2017. 5
- [35] Jianxiong Xiao, James Hays, Krista A Ehinger, Aude Oliva, and Antonio Torralba. Sun database: Large-scale scene recognition from abbey to zoo. In *CVPR*, pages 3485–3492. IEEE, 2010. 5
- [36] Lingxiao Yang, Ru-Yuan Zhang, Yanchen Wang, and Xiaohua Xie. Mma: Multi-modal adapter for vision-language models. In *CVPR*, pages 23826–23837, 2024. 3, 6
- [37] Hantao Yao, Rui Zhang, and Changsheng Xu. Visual-language prompt tuning with knowledge-guided context optimization. In *CVPR*, pages 6757–6767, 2023. 3, 8
- [38] Hantao Yao, Rui Zhang, and Changsheng Xu. Tcpr: Textual-based class-aware prompt tuning for visual-language model. In *CVPR*, pages 23438–23448, 2024. 3, 6
- [39] Lewei Yao, Runhui Huang, Lu Hou, Guansong Lu, Minzhe Niu, Hang Xu, Xiaodan Liang, Zhenguo Li, Xin Jiang, and Chunjing Xu. Filip: Fine-grained interactive language-image pre-training. *arXiv preprint arXiv:2111.07783*, 2021. 2
- [40] Lu Yuan, Dongdong Chen, Yi-Ling Chen, Noel Codella, Xiyang Dai, Jianfeng Gao, Houdong Hu, Xuedong Huang, Boxin Li, Chunyuan Li, et al. Florence: A new foundation model for computer vision. *arXiv preprint arXiv:2111.11432*, 2021. 2
- [41] Yuhang Zang, Wei Li, Kaiyang Zhou, Chen Huang, and Chen Change Loy. Open-vocabulary detr with conditional matching. In *ECCV*, pages 106–122. Springer, 2022. 3
- [42] Ji Zhang, Shihan Wu, Lianli Gao, Heng Tao Shen, and Jingkuan Song. Dept: Decoupled prompt tuning. In *CVPR*, pages 12924–12933, 2024. 3
- [43] Renrui Zhang, Rongyao Fang, Wei Zhang, Peng Gao, Kunchang Li, Jifeng Dai, Yu Qiao, and Hongsheng Li. Tip-adapter: Training-free clip-adapter for better vision-language modeling. *arXiv preprint arXiv:2111.03930*, 2021. 3
- [44] Renrui Zhang, Wei Zhang, Rongyao Fang, Peng Gao, Kunchang Li, Jifeng Dai, Yu Qiao, and Hongsheng Li. Tip-adapter: Training-free adaption of clip for few-shot classification. In *ECCV*, pages 493–510. Springer, 2022. 1
- [45] Yi Zhang, Meng-Hao Guo, Miao Wang, and Shi-Min Hu. Exploring regional clues in clip for zero-shot semantic segmentation. In *CVPR*, pages 3270–3280, 2024. 3
- [46] Yi Zhang, Ce Zhang, Ke Yu, Yushun Tang, and Zhihai He. Concept-guided prompt learning for generalization in vision-language models. In *AAAI*, pages 7377–7386, 2024. 1, 3
- [47] Yiwu Zhong, Jianwei Yang, Pengchuan Zhang, Chunyuan Li, Noel Codella, Liunan Harold Li, Luowei Zhou, Xiyang Dai, Lu Yuan, Yin Li, et al. Regionclip: Region-based language-image pretraining. In *CVPR*, 2022. 3
- [48] Chong Zhou, Chen Change Loy, and Bo Dai. Extract free dense labels from clip. In *ECCV*, pages 696–712. Springer, 2022. 3
- [49] Kaiyang Zhou, Jingkang Yang, Chen Change Loy, and Ziwei Liu. Conditional prompt learning for vision-language models. In *CVPR*, pages 16816–16825, 2022. 1, 3, 6
- [50] Kaiyang Zhou, Jingkang Yang, Chen Change Loy, and Ziwei Liu. Learning to prompt for vision-language models. *IJCV*, 130(9):2337–2348, 2022. 1, 3, 5, 6, 8
- [51] Xingyi Zhou, Rohit Girdhar, Armand Joulin, Philipp Krähenbühl, and Ishan Misra. Detecting twenty-thousand classes using image-level supervision. In *ECCV*, pages 350–368. Springer, 2022. 3
- [52] Beier Zhu, Yulei Niu, Yucheng Han, Yue Wu, and Hanwang Zhang. Prompt-aligned gradient for prompt tuning. In *ICCV*, pages 15659–15669, 2023. 3